

## ATTENUATION OF VHE GAMMA RAYS BY THE MILKY WAY INTERSTELLAR RADIATION FIELD

IGOR V. MOSKALENKO<sup>1</sup>

Hansen Experimental Physics Laboratory, Stanford University, Stanford, CA 94305

TROY A. PORTER

Department of Physics and Astronomy, Louisiana State University, Baton Rouge, LA 70803

AND

ANDREW W. STRONG

Max-Planck-Institut für extraterrestrische Physik, Postfach 1312, D-85741 Garching, Germany

*Submitted 2005 November 2; accepted 2006 February 17*

## ABSTRACT

The attenuation of very high energy  $\gamma$ -rays by pair production on the Galactic interstellar radiation field has long been thought of as negligible. However, a new calculation of the interstellar radiation field consistent with multi-wavelength observations by DIRBE and FIRAS indicates that the energy density of the Galactic interstellar radiation field is higher, particularly in the Galactic center, than previously thought. We have made a calculation of the attenuation of very high energy  $\gamma$ -rays in the Galaxy using this new interstellar radiation field which takes into account its nonuniform spatial and angular distributions. We find that the maximum attenuation occurs around 100 TeV at the level of about 25% for sources located at the Galactic center, and is important for both Galactic and extragalactic sources.

*Subject headings:* Galaxy: general — gamma-rays: observations — gamma-rays: theory — radiation mechanisms: general — radiative transfer

## 1. INTRODUCTION

The attenuation of very high energy (VHE)  $\gamma$ -rays by pair production on the Galactic interstellar radiation field (ISRF) has previously been considered to be negligible (Nikishov 1962; Protheroe 1986). The main contribution is thought to come from pair production on the cosmic microwave background (CMB) where the effective threshold for attenuation is  $\sim 100$  TeV and a maximum is reached at about 2000 TeV, currently accessible only via air-shower experiments. The Galactic ISRF photons are more energetic so that the effective threshold is lower ( $\sim 100$  GeV) and the attenuation increases slowly to a maximum around 100 TeV. This covers the energy range of present day Imaging Atmospheric Cherenkov Telescopes, such as the HESS instrument. A rough estimate of the attenuation of VHE  $\gamma$ -rays coming from the Galactic center (GC), which uses a new ISRF (Porter & Strong 2005), but assumes an isotropic angular distribution for the ISRF, shows that the effect is observable (Zhang et al. 2005). Given the essential anisotropy of the Galactic ISRF with most of the photons going outwards from the inner Galaxy, the effect depends on the position of the source of VHE photons and its orientation relative to the observer in the Galactic plane. We calculate the attenuation of VHE  $\gamma$ -rays due to pair production with the Galactic photon field using the total ISRF over the entire Galaxy on a fine spatial grid which takes into account the nonuniform spatial and anisotropic angular distribution of background photons.

## 2. INTERSTELLAR RADIATION FIELD

The essential ingredients to calculate the Galactic ISRF are a model for the distribution of stars in the Galaxy, a model for the dust distribution and properties, and a treatment of scattering, absorption, and subsequent re-emission of the stellar light by the dust. We briefly describe our ISRF calculation, which is a further development of the work reported by Porter & Strong (2005); full details will be given in a forthcoming paper (Porter & Strong, in preparation).

Our stellar model assumes a type classification based on that used in the SKY model of Wainscoat et al. (1992). It includes 87 stellar classes encompassing main sequence stars, AGB stars and exotics. For each stellar type there is a local star number density, scale height above the plane, fraction of local number density in each of several discrete spatial components, and spectrum in standard photometric filters. The stars are distributed in seven geometrical components: thin and thick disc, halo, bulge, bar, ring, and spiral arms. Spectra for normal stars are taken from the synthetic spectral library of Girardi et al. (2002). Spectra for AGB stars and exotics are as given in the SKY model.

We assume a dust model including graphite, polycyclic aromatic hydrocarbons (PAHs), and silicate. Dust grains in the model are spherical and the absorption and scattering efficiencies for graphite, PAHs, and silicate grains are taken from Li & Draine (2001). The grain model abundance and size distribution are taken from Weingartner & Draine (2001) (their best fit Milky Way model), and a purely neutral interstellar medium is assumed. We consider only coherent scattering, and a Henyey-Greenstein angular distribution function (Henyey & Greenstein 1941) is used in the scattering cal-

<sup>1</sup> Also Kavli Institute for Particle Astrophysics and Cosmology, Stanford University, Stanford, CA 94309

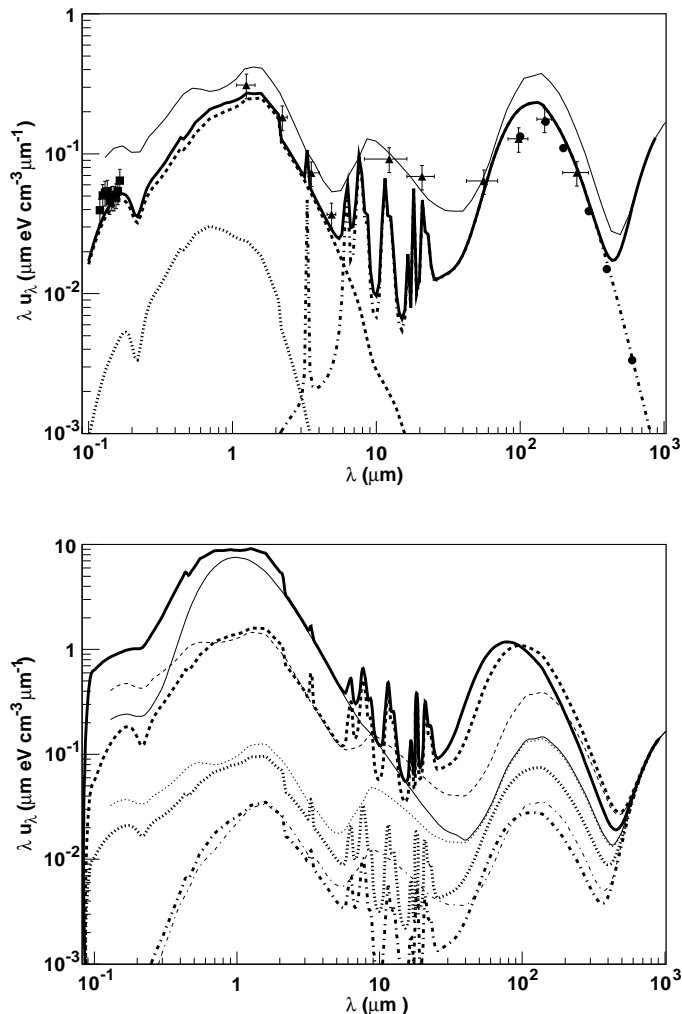


FIG. 1.— Interstellar radiation field energy density. Local interstellar radiation field (upper): heavy solid line, total radiation field including CMB; heavy dashed line, contribution by stars; heavy dotted line, scattered light; heavy dot-dashed line, infrared; thin solid line, local ISRF from Strong, Moskalenko & Reimer (2000). Data: squares, Apollo (Henry, Anderson & Fastie 1980); triangles, DIRBE (Arendt, et al. 1998); circles, FIRAS (Finkbeiner, Davis & Schlegel 1999). Interstellar total radiation field radial variation (lower): solid line,  $(R, z) = (0 \text{ kpc}, 0 \text{ kpc})$ ; dashed line,  $(R, z) = (4 \text{ kpc}, 0 \text{ kpc})$ ; dotted line,  $(R, z) = (12 \text{ kpc}, 0 \text{ kpc})$ ; dash-dotted line,  $(R, z) = (16 \text{ kpc}, 0 \text{ kpc})$ . Heavy lines are for our ISRF; thin lines for the ISRF of Strong, Moskalenko & Reimer (2000).

calculation. The stochastic heating of grains smaller than  $\sim 0.1 \mu\text{m}$  is treated using the “thermal continuous” approach of Draine & Li (2001); we calculate the equilibrium heating of larger dust grains by balancing absorption with re-emission as described by Li & Draine (2001).

Dust is assumed to follow the Galactic gas distribution. We use the gas model for neutral and molecular hydrogen given by Moskalenko et al. (2002). The radial variation in the Galactic metallicity gradient is taken to be 0.07 dex/kpc (Strong et al. 2004, and references therein).

A cylindrical geometry is adopted for the radiation field calculation. Our calculations are simplified by assuming symmetry in azimuth and about the Galactic plane. The maximum radial extent is taken to be  $R_{\text{max}} = 20 \text{ kpc}$ . The maximum height above the Galac-

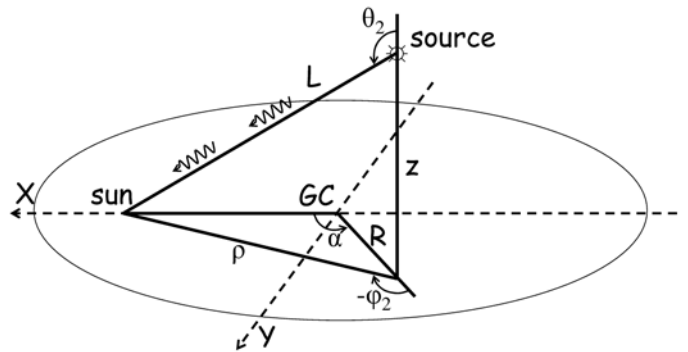


FIG. 2.— Angles involved in the calculation:  $(R, z, \alpha)$ , galactocentric coordinates of the source of VHE photons;  $(\theta_2, \phi_2)$ , angles of the VHE photon; GC marks the Galactic center; and the observer’s position is marked by “sun”.

tic plane is taken to be  $z_{\text{max}} = 5 \text{ kpc}$ . The Sun is located at  $R_S = 8.5 \text{ kpc}$  from the GC. The Galaxy is divided into elements of equal volume and the total radiation field is calculated for each.

The radiation field from stellar and scattered light is obtained using a modified form of the so-called partial intensity method (Baes & Dejonghe 2001). Henceforth, we will refer to the total stellar and scattered light as the “optical” radiation field. The infra-red radiation field is obtained by using the optical radiation field to calculate the dust emissivity for stochastic and equilibrium heating. The dust emission is integrated to obtain the infra-red radiation field throughout the Galaxy.

Fig. 1 (upper panel) shows our calculated local ISRF including the CMB; also shown in the figure is the local ISRF calculated by Strong, Moskalenko & Reimer (2000). The agreement of our computed ISRF with the data is generally good. We note that our new ISRF provides an improved fit to the observations around  $100 \mu\text{m}$  compared to the earlier model of Strong, Moskalenko & Reimer (2000). This is particularly important for our optical depth calculation, since the majority of the attenuation is on these more numerous less-energetic photons of the ISRF.

Fig. 1 (lower panel) shows the radial variation in the Galactic plane of our ISRF (thick lines) together with that of Strong, Moskalenko & Reimer (2000) (thin lines). Toward the inner Galaxy, our ISRF predicts a significantly higher energy density than previously described, particularly for the infra-red component. This arises because of the coupling between the optical radiation field and the infra-red emission: in our calculation, the optical radiation field is used as direct input to the dust heating calculation, which was not done in previous work. The intense optical radiation field toward the inner Galaxy heats the dust to warmer temperatures, increasing the emission in the infra-red. Even though the optical emission does not cause a direct enhancement to the attenuation at GeV to TeV energies – the energy of these photons is typically a few eV, lowering the threshold, however their number density is too low to provide significant absorption – it is essential to calculate this component of the ISRF to obtain the correct emission and angular distribution for the infra-red. Further discussion of the new ISRF is deferred to a forthcoming paper (Porter & Strong, in preparation).

## 3. CALCULATIONS

The optical depth for VHE  $\gamma$ -rays is given by the general formula:

$$\tau_{\gamma\gamma}(E) = \int_L dx \int d\varepsilon \int d\Omega_1 \frac{dN(\varepsilon, \Omega_1, x)}{d\varepsilon d\Omega_1} \sigma_{\gamma\gamma}(\varepsilon_c) (1 - \cos\theta), \quad (1)$$

where  $dN(\varepsilon, \Omega_1, x)/d\varepsilon d\Omega_1$  is the differential number density of background photons at the point  $x$ ,  $\varepsilon$  is the background photon energy,  $d\Omega_1 = d\cos\theta_1 d\phi_1$  is a solid angle,  $\sigma_{\gamma\gamma}$  is the total cross section for the pair production process  $\gamma\gamma \rightarrow e^+e^-$  (Jauch & Rohrlich 1980),  $\varepsilon_c = [\frac{1}{2}\varepsilon E(1 - \cos\theta)]^{1/2}$  is the center-of-momentum system energy of a photon, and  $\theta$  is the angle between the momenta of the two photons in the observer's frame. The integral over  $x$  should be taken along the path of the  $\gamma$ -rays from the source to the observer.

The ISRF is cylindrically symmetric so that the photon angular distribution depends on  $R$  and  $z$  only. In Fig. 2 we illustrate the galactocentric coordinate system  $(R, z, \alpha)$ . To calculate  $\cos\theta$ , the polar and azimuthal angles of the VHE photon,  $\theta_2$  and  $\phi_2$ , are derived:

$$\begin{aligned} \rho^2 &= R^2 + R_s^2 - 2RR_s \cos\alpha, \\ \begin{cases} \sin\phi_2 = -(R_s/\rho) \sin\alpha, \\ \cos\phi_2 = -(\rho^2 + R^2 - R_s^2)/2R\rho, \end{cases} \\ \begin{cases} \sin\theta_2 = \rho(\rho^2 + z^2)^{-1/2}, \\ \cos\theta_2 = -(1 - \sin^2\theta_2)^{1/2}, \end{cases} \\ \cos\theta &= \cos\theta_1 \cos\theta_2 + \sin\theta_1 \sin\theta_2 \cos(\phi_1 - \phi_2), \end{aligned} \quad (2)$$

where  $R_s$  is the galactocentric radius of the Sun. The integration of eq. (1) is done numerically.

For the calculation of the optical depth in the CMB field we use the formula:

$$\tau_{\gamma\gamma}^{CMB}(E) = \frac{-4kT}{(\hbar c)^3 \pi^2 E^2} \int_L dx \int_{m_e c^2}^{\infty} d\varepsilon \varepsilon_c^3 \sigma_{\gamma\gamma}(\varepsilon_c) \log\left(1 - e^{-\varepsilon_c^2/EkT}\right), \quad (3)$$

where  $kT$  is the CMB temperature, and  $m_e c^2$  is the electron rest mass.

## 4. RESULTS

Fig. 3 shows the attenuation for selected positions  $(R, z, \alpha)$  as a function of incident  $\gamma$ -ray energy. For sources located at the GC the attenuation is  $\sim 12\%$  at 30 TeV and  $\sim 23\%$  at 100 TeV. In Table 1 we give our optical depth results for selected values of  $R$  and  $z$  for  $\alpha = 0^\circ, 90^\circ$  and  $180^\circ$  at 30 and 100 TeV without contribution by the CMB. The attenuation is strongest for VHE  $\gamma$ -ray sources located toward the inner Galaxy and on its farside.

To illustrate the effect of the anisotropic radiation field on the attenuation calculation, we show in Fig. 4 the ratio of the optical depths  $\tau_{\gamma\gamma}/\tau_{\gamma\gamma}^{\text{iso}}$ , where  $\tau_{\gamma\gamma}$  is calculated using the full angular distribution of the ISRF and  $\tau_{\gamma\gamma}^{\text{iso}}$  is calculated assuming an isotropic distribution, for a source located at  $z = 0$  kpc (upper panel) and  $z = 5$  kpc (lower panel) emitting 100 TeV  $\gamma$ -rays as a function of position. The variation of  $\tau_{\gamma\gamma}/\tau_{\gamma\gamma}^{\text{iso}}$  over the Galaxy as seen from Earth is non-trivial. For sources located

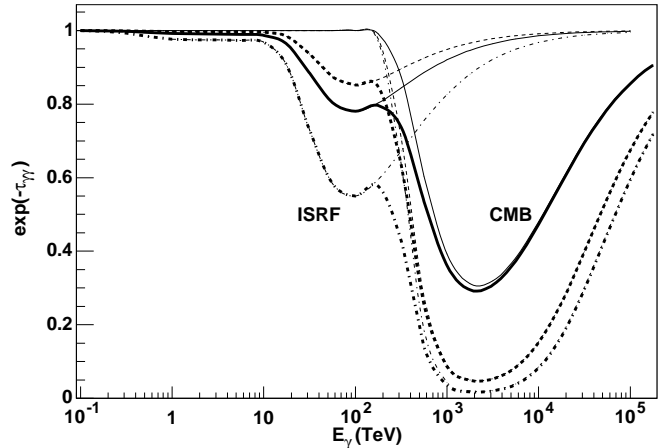


FIG. 3.— Transmittance of VHE  $\gamma$ -rays as a function of  $\gamma$ -ray energy. Solid line:  $(R, z, \alpha) = (0 \text{ kpc}, 0 \text{ kpc}, 0^\circ) - L = 8.5 \text{ kpc}$ ; Dashed line:  $(R, z, \alpha) = (20 \text{ kpc}, 0 \text{ kpc}, 90^\circ) - L = 21.8 \text{ kpc}$ ; Dash-dotted line:  $(R, z, \alpha) = (20 \text{ kpc}, 0 \text{ kpc}, 180^\circ) - L = 28.5 \text{ kpc}$ . Thick lines give the total transmittance curve including the ISRF and CMB. Left-most thin lines give the transmittance for the ISRF only; right-most thin lines for the CMB only.

TABLE 1  
OPTICAL DEPTH  $\tau_{\gamma\gamma}$  AT 30 AND 100 TeV

R, kpc	z, kpc	30 TeV			100 TeV		
		$\alpha = 0^\circ$	$90^\circ$	$180^\circ$	$\alpha = 0^\circ$	$90^\circ$	$180^\circ$
0	0	0.12	...	...	0.25	...	...
5	0	0.01	0.15	0.22	0.05	0.32	0.41
10	0	0.01	0.08	0.28	0.02	0.21	0.54
15	0	0.02	0.07	0.31	0.05	0.18	0.58
20	0	0.03	0.07	0.32	0.06	0.16	0.60
0	5	0.03	...	...	0.09	...	...
5	5	0.01	0.04	0.06	0.05	0.10	0.15
10	5	0.02	0.05	0.09	0.04	0.12	0.21
15	5	0.03	0.05	0.12	0.05	0.13	0.26
20	5	0.03	0.06	0.14	0.06	0.13	0.29

in the Galactic plane between the GC and solar system the ratio is less than one since the majority of the ISRF photons are coming from the GC direction,  $\cos\theta \rightarrow 1$  in eq. (1) and the interactions are mainly following, leading to a lower pair production probability when the ISRF angular distribution is taken into account. The reverse situation,  $\tau_{\gamma\gamma}/\tau_{\gamma\gamma}^{\text{iso}} > 1$ , occurs for  $\gamma$ -rays interacting with the ISRF in the outer Galaxy, where the majority of interactions are now head-on,  $\cos\theta \rightarrow -1$  in eq. (1). For sources located beyond the GC, the ratio is  $\sim 1$ . The interpretation of this case is straightforward:  $\gamma$ -rays emitted on the farside of the Galaxy toward the solar system have mainly head-on absorption interactions until they reach the GC, whereupon the interactions become mainly following. The isotropic case averages the angular distribution, and therefore leads to  $\tau_{\gamma\gamma}/\tau_{\gamma\gamma}^{\text{iso}} \sim 1$ . We note that the optical depth ratio increases monotonically with  $z$ , and is a result of the progressively more head-on nature of the  $\gamma$ -ray absorption interactions for sources located at larger distances from the plane.

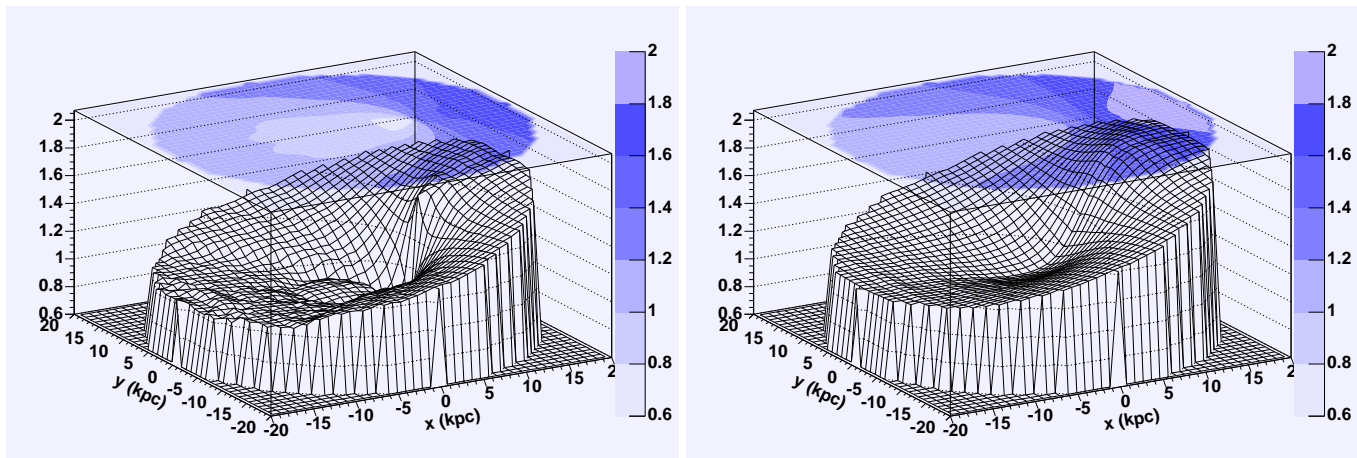


FIG. 4.— Effect of anisotropic ISRF on optical depth calculation at 100 TeV. Shown is the ratio of the optical depths  $\tau_{\gamma\gamma}/\tau_{\gamma\gamma}^{iso}$  as a function of position  $(x, y)$  for a source located at  $z = 0$  kpc (left) and  $z = 5$  kpc (right). The solar system is located at  $(x, y) = (8.5$  kpc, 0 kpc), exactly where the optical depth ratio rises sharply.

Our results show that the attenuation of VHE  $\gamma$ -rays by the Galactic radiation field may be marginally observable by the HESS instrument which has an effective sensitivity up to several tens of TeV (Aharonian et al. 2005). The attenuation of VHE  $\gamma$ -rays from the sources on the Galaxy’s farside will essentially steepen their spectra above  $\sim 10$  TeV. In any case correction of source spectra for absorption is required. Interestingly, observations by future high energy experiments of the steepening of

the spectra of Galactic sources in the GC region and beyond may serve as a probe of the Galactic ISRF.

I. V. M. acknowledges partial support from NASA Astronomy and Physics Research and Analysis Program (APRA) grant. T. A. P. acknowledges partial support from the US Department of Energy.

#### REFERENCES

- Aharonian, F., et al., 2005, ApJ, accepted (astro-ph/0510397)  
 Arendt, R. G., et al., 1998, ApJ, 508, 74  
 Baes, M. & Dejonghe, H., 2001, MNRAS, 326, 722  
 Draine, B. T. & Li, A., 2001, ApJ, 551, 807  
 Finkbeiner, D., Davis, M. & Schlegel, D. J., 1999, ApJ, 524, 867  
 Freudenreich, H. T., 1998, ApJ, 492, 495  
 Girardi, L., et al., 2002, A&A, 391, 195  
 Henry, R. C., Anderson, R. C., & Fastie, W. G., 1980, ApJ, 239, 859  
 Henyey, L. G. & Greenstein, J. L., 1941, ApJ, 93, 70  
 Jauch, J. M., & Rohrlich, F., 1980, Theory of Photons and Electrons (New York: Springer-Verlag)  
 Li, A. & Draine, B. T., 2001, ApJ, 554, 778  
 Moskalenko, I. V., Strong, A. W., Ormes, J. F., & Potgieter, M. S., 2002, ApJ, 565, 280  
 Nikishov, A. I., 1962, Soviet Physics JETP, 14, 393  
 Porter, T. A. & Strong, A. W., 2005, in Proc. 29<sup>th</sup> Int. Cosmic Ray Conf. (Pune) (astro-ph/0507119)  
 Protheroe, R. J., 1986, MNRAS, 221, 769.  
 Strong, A. W., Moskalenko, I. V., & Reimer, O., 2000, ApJ, 537, 763  
 Strong, A. W., Moskalenko, I. V., Reimer, O., Digel, S. & Diehl, R., 2004, A&A, 422, L47  
 Wainscoat, R. J., et al., 1992, ApJS, 83, 111  
 Weingartner, J. C. & Draine, B. T., 2001, ApJ, 548, 296  
 Zhang, J.-L., Bi, X.-J., & Hu, H.-B. 2005, preprint (astro-ph/0508236)